

Table EA-1. Empirical bond-valences for Mn-Zn precipitate^a.

	O1 ^b	O1 ^c	O1 ^d	O1 ^e	O2, O3	O3	O4	Σ	Formal valence
Mn1	0.628 ×6→ ×3↓	0.628 ×2↓	0.628 ×2↓	0.628 ×2↓				3.8	4
Mn2, Mn3		0.469 ×3→			0.433 ×3→			2.7	3
Zn1			0.403 ×3→			0.372 ×3→		2.3	2
Zn2				0.731 ×3→			0.543	2.7	2
H ⁺	0.11 ^f								
Σ	1.9 – 2.0 ^g	1.7	1.7	2.0					

^(a) Bond valences in valence unit (v.u.) were calculated using the Valence for Dos program (v. 2.0 - http://www.ccp14.ac.uk/solution/bond_valence/index.html) and the parameters from Brese and O' Keeffe (1991).

^(b) O1 coordinated to 3 Mn⁴⁺ in Mn1 (Table 1).

^(c) O1 coordinated to 2 Mn⁴⁺ in Mn1 and 1 Mn³⁺ in Mn2 or Mn3.

^(d) O1 coordinated to 2 Mn⁴⁺ in Mn1 and 1 Zn²⁺ in Zn1.

^(e) O1 coordinated to 2 Mn⁴⁺ in Mn1 and 1 Zn²⁺ in Zn2.

^(f) O5-H-O1 H-bond.

^(g) Depending on whether this O1 receives additional valence from H⁺ through H-bond.

REFERENCE: Brese N.E. and O' Keeffe M. (1991) Bond-valence parameters for solids. *Acta Crystallogr.* **B47**, 192-197.

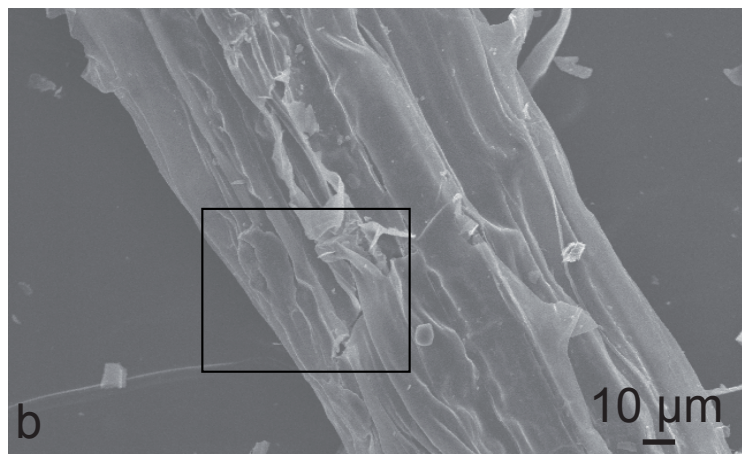
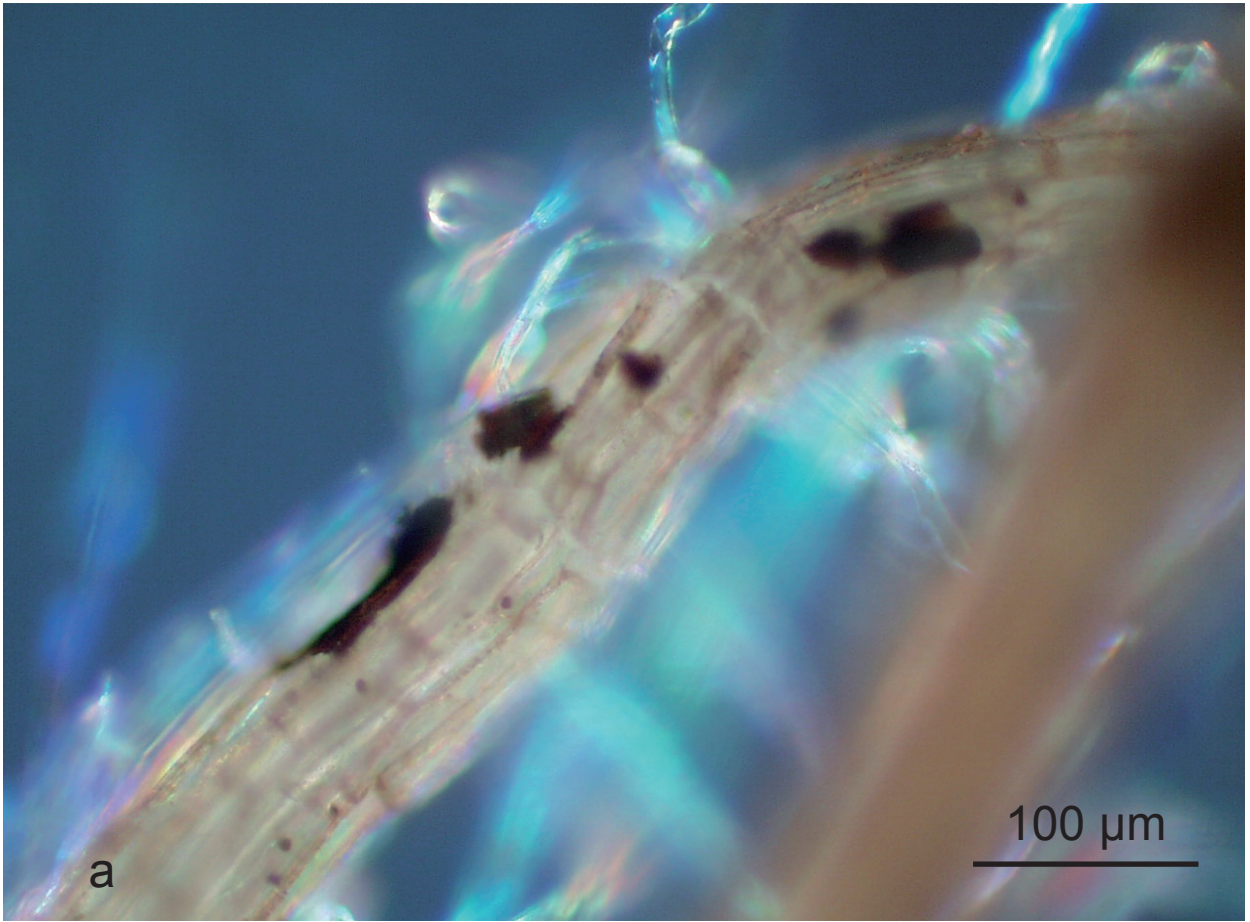


Fig. EA-1: Roots of *Festuca rubra* grown on a Zn-contaminated sediment. (a) Close-up photograph from Fig. 1a. (b) Lower magnification of Fig. 1c.

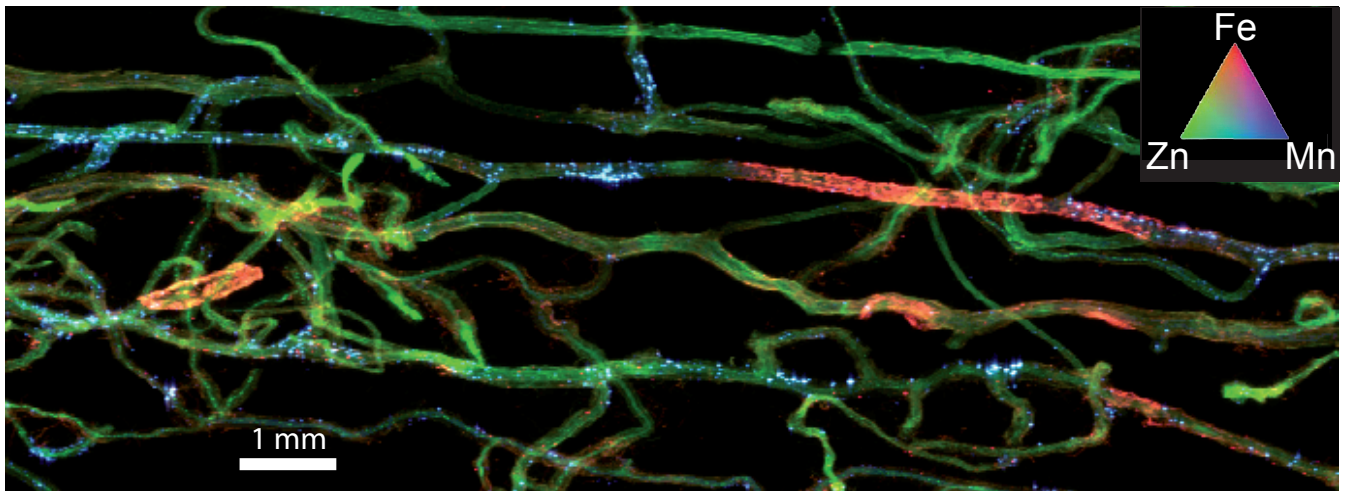


Fig. EA-2: Tricolor (RGB) μ -XRF map of a bundle of roots. Red codes for Fe, green for Zn, and blue for Mn. Each pixel is colored in proportion to Fe-, Zn- and Mn- $K\alpha$ signals. Pixel size is $18 \times 15 \mu\text{m}^2$.

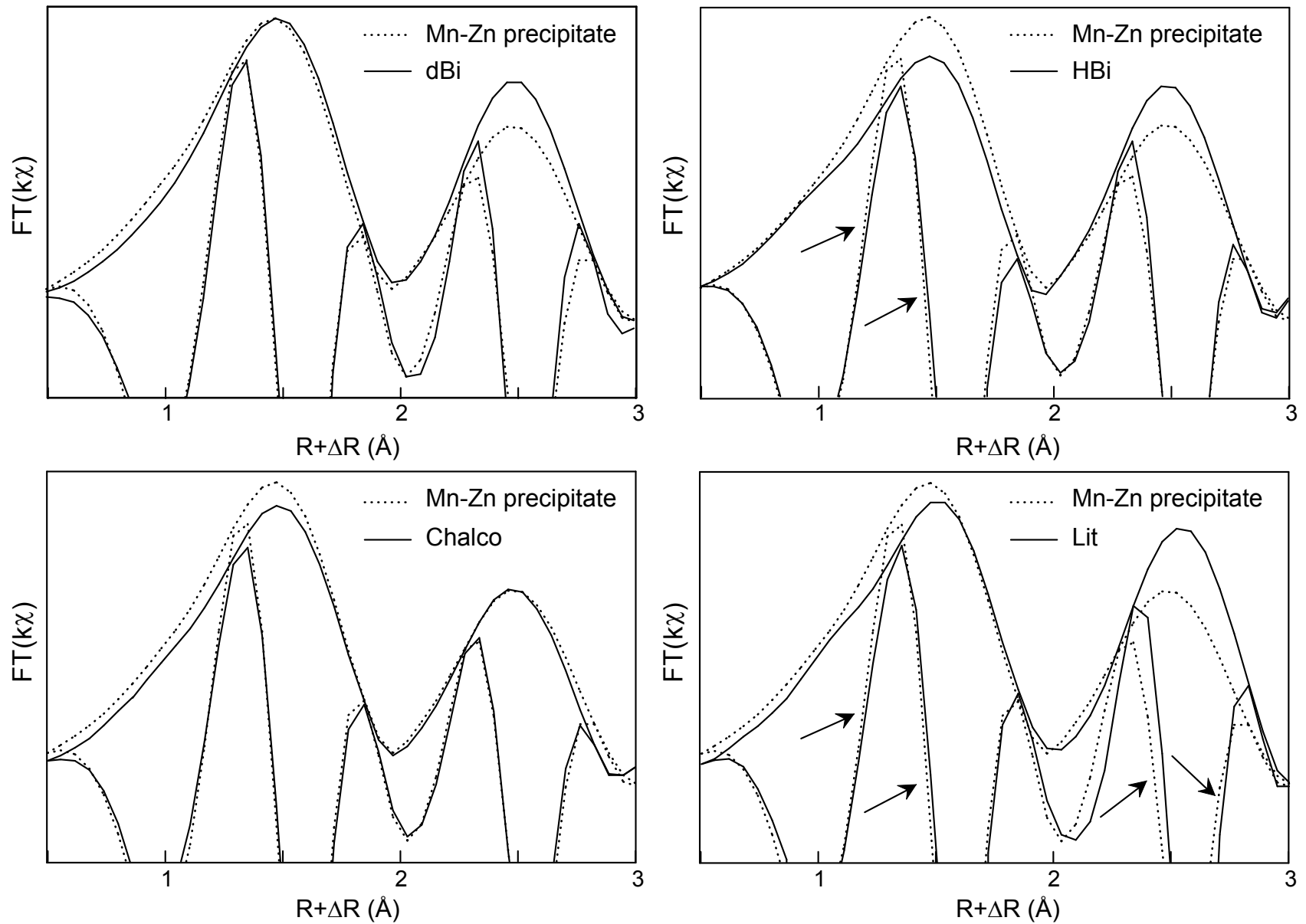


Fig. EA-3: Fourier transforms (FTs) of the manganese K-edge k -weighted EXAFS spectra for the Mn-Zn root precipitate and synthetic ^{VI}Zn -sorbed $\delta\text{-MnO}_2$ (dBi, synthetic turbostratic birnessite), chalcophanite (Chalco), hexagonal birnessite (HBi), and lithiophorite (Lit). Expansion of the [1-3 Å] $R+\Delta R$ interval.

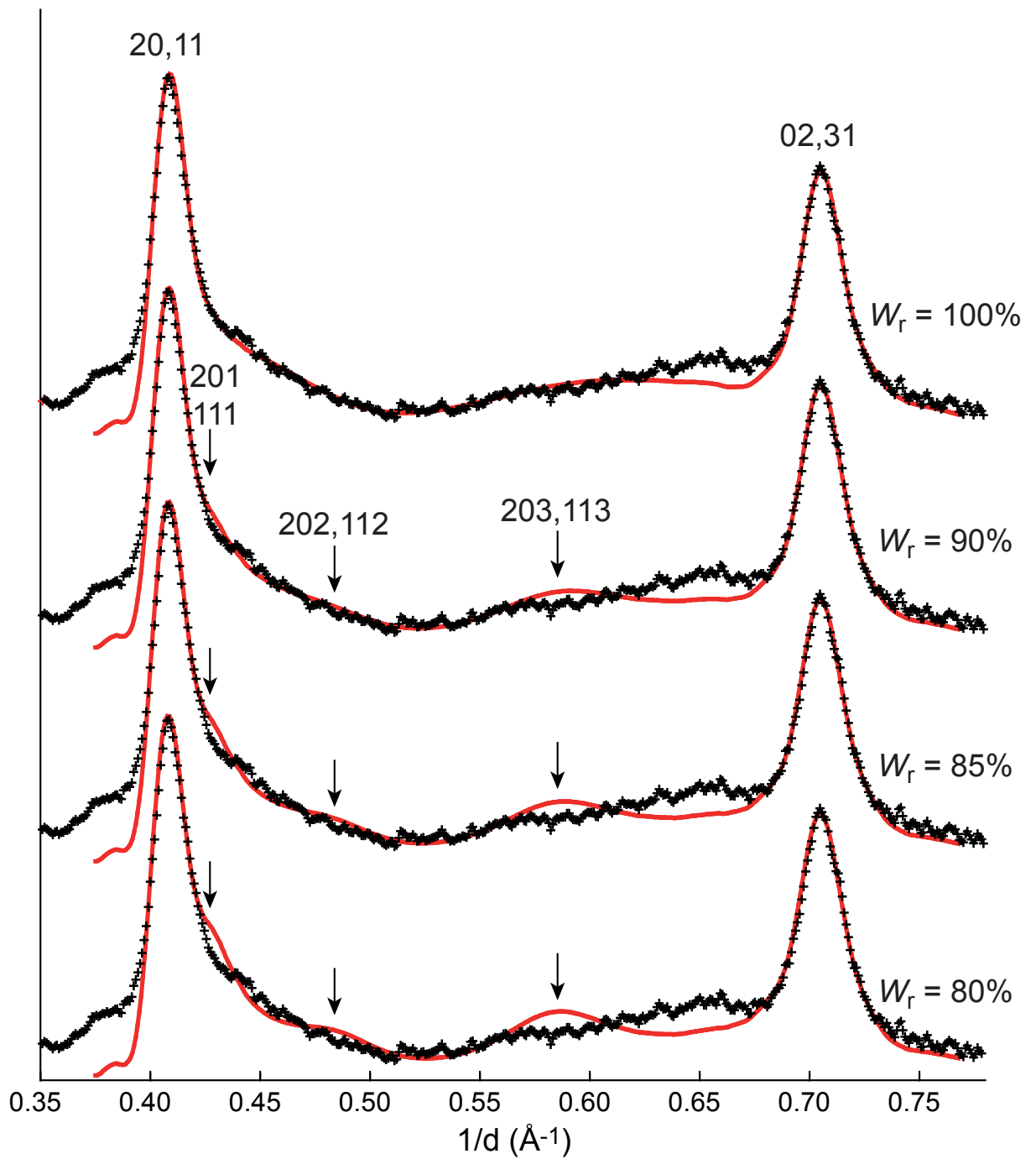


Fig. EA-4: Simulations of the [20,11] and [02,31] X-ray scattering bands (black crosses, C-centered layer cell). Intensities (red lines) were calculated for the optimal structure model (Table 1) with different occurrence probabilities of random stacking faults (W_r). Arrows indicate the positions of hkl reflections.

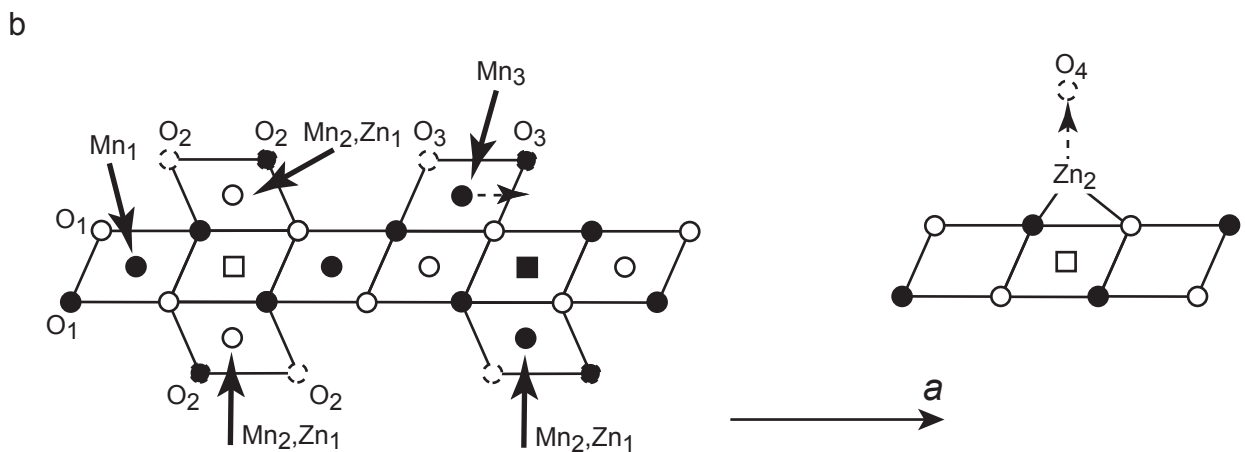
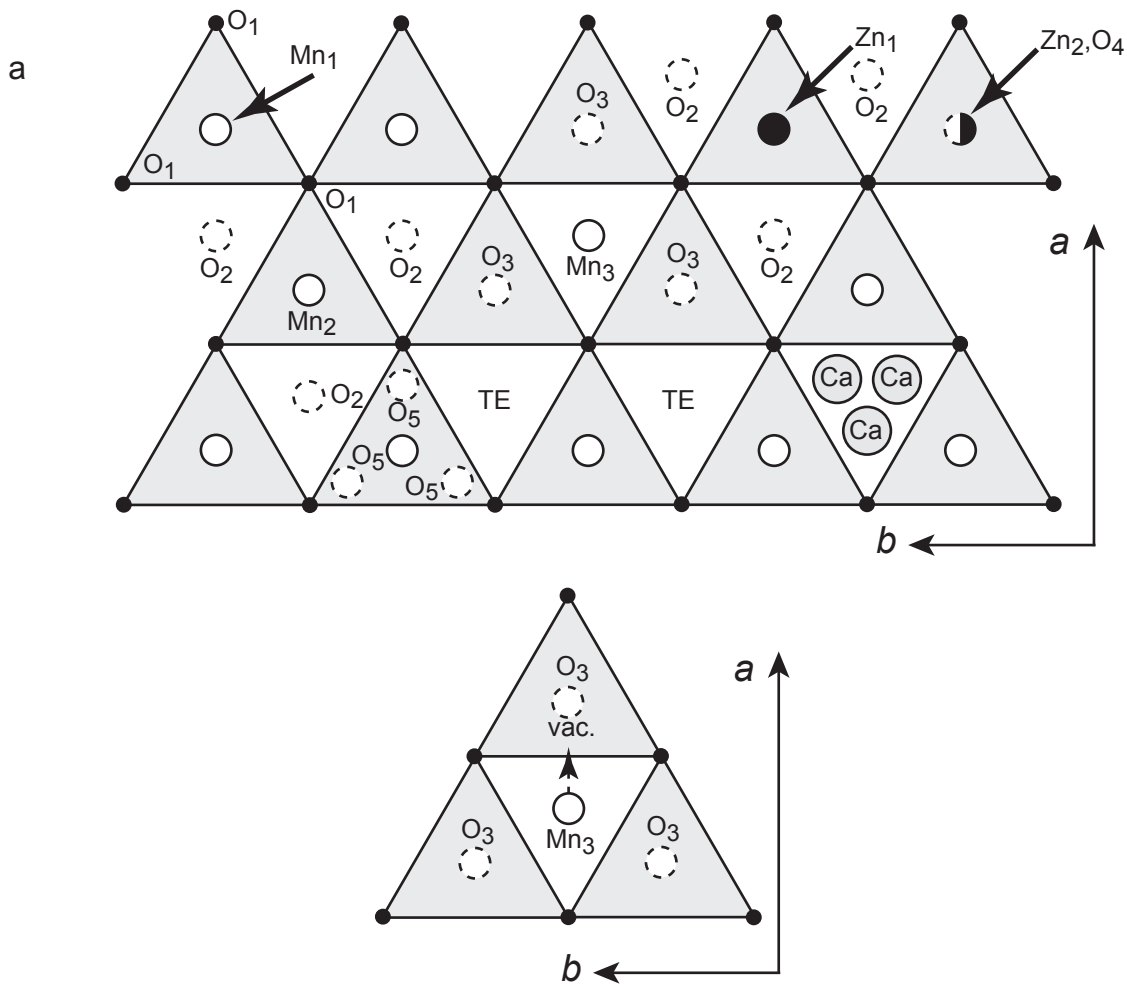


Fig. EA-5: Idealized structure of Mn-Zn precipitate. (a) Projection on the ab plane. The upper surface of the layer is shown as light shaded triangles, and the atomic notations are the same as in Table 1. (b) Projection along the b axis. Open and solid symbols indicate atoms at $y = 0$ and $y = \pm\frac{1}{2}$, respectively. Squares represent vacant layer octahedra. The Mn_3 and Zn_2 atoms can be shifted from their positions as indicated by the dashed arrows to obtain more realistic interatomic distances (see Table EA-1).

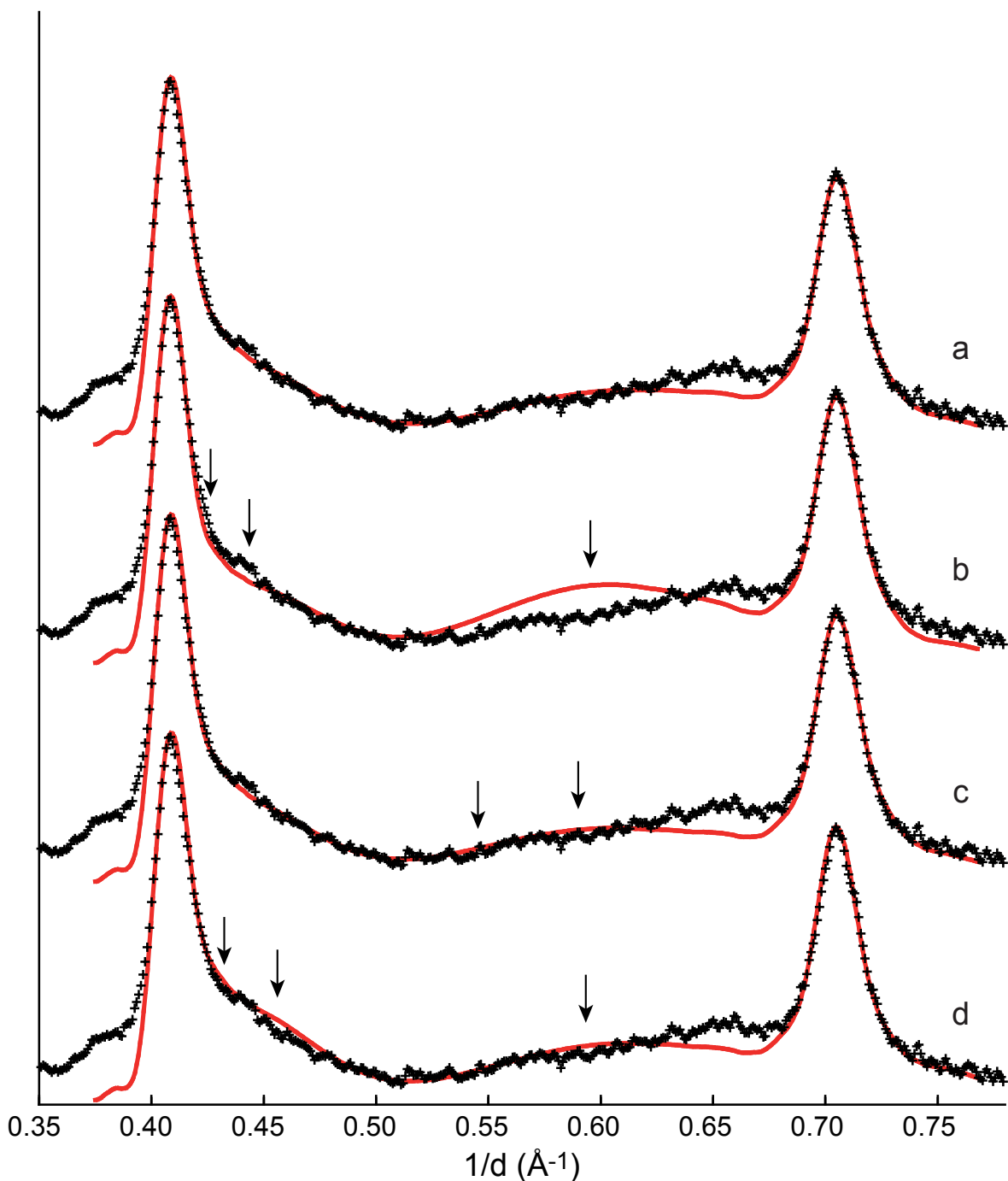


Fig. EA-6: Simulations of the [20,11] and [02,31] X-ray scattering bands (C-centered layer cell, black crosses). Small but significant misfits between experimental and calculated patterns are pointed out with arrows. Intensities (red lines) were calculated with a turbostratic layer stacking (no interlayer correlation). (a) Optimal model (Table 1; Figs. 8 and EA-5); $R_{wp} = 3.49\%$. (b) Model with ^{IV}Zn (Zn2) in (0, 0, 1.97 Å), instead of (0, 0, 1.77 Å) in the optimal fit, so as to increase the Zn-O bond length from 1.82 Å (Table 2) to 1.91 Å. Coordinated H_2O molecules (O4) were moved from (0, 0, 3.70 Å) to (0, 0, 3.90 Å); $R_{wp} = 3.92\%$. (c) Model with ^{VI}Zn (Zn1) in (0, 0, 2.30 Å), instead of (0, 0, 2.20 Å) in the optimal fit so as to decrease the sum valence of Zn1 from 2.3 (Table EA-1) to 2.0. Coordinated H_2O molecules (O2) were moved from (-0.333, 0, 3.45 Å) to (-0.333, 0, 3.65 Å); $R_{wp} = 3.55\%$. (d) Model with Ca in (-0.333, 0, 3.60 Å), instead of (-0.410, 0, 3.60 Å) and equivalent positions in the optimal fit; $R_{wp} = 3.51\%$. Unless specified, all parameters used in calculations are those of the optimal model.

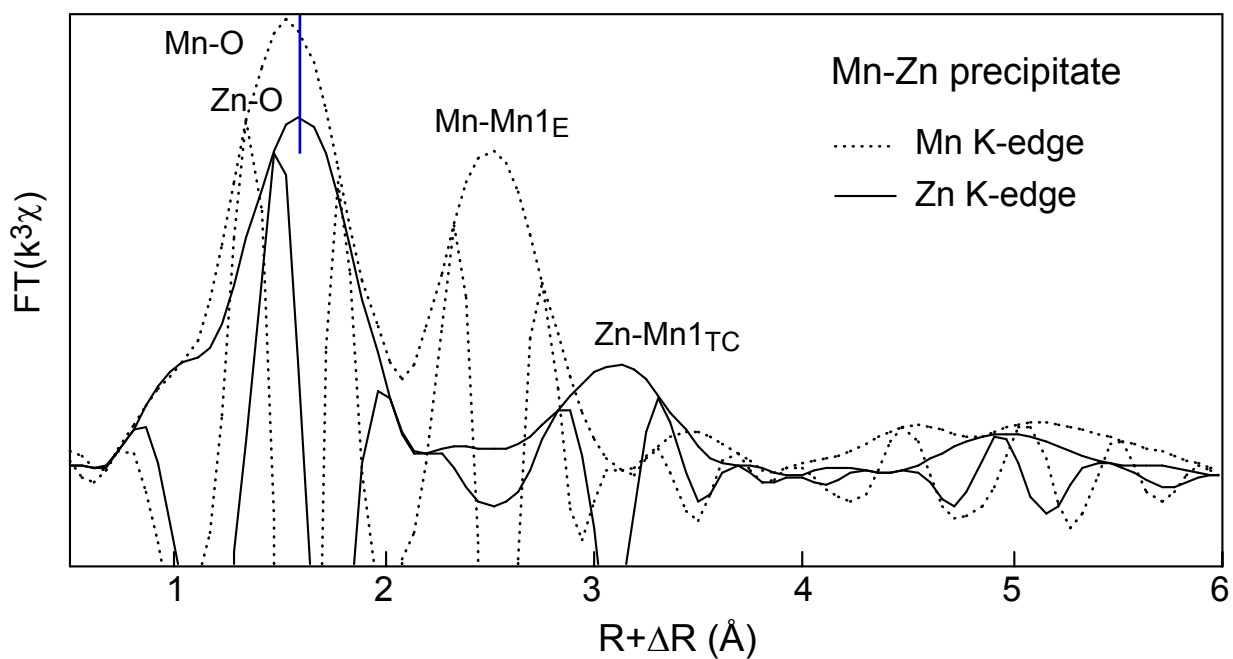


Fig. EA-7: Fourier transform of the EXAFS spectra for the Mn-Zn precipitate at the Mn and Zn K-edges. The average Mn-O and Zn-O EXAFS distances (R values) are 1.90 Å and 2.00 Å, respectively.